Proceedings of the 17th International Symposium on the
Packaging and Transportation of Radioactive Materials
PATRAM 2013
August 18-23, 2013, San Francisco, CA, USA

Demonstration of the Structural Performance of Ensa's ENUN 52B in a Range of Impact Scenarios in Storage and Transportation

Chi-Fung Tso Arup, UK
Kevin Ip Arup, UK
Sundip Shah Arup, UK
Matthew Walden Arup, UK

David Garrido Ensa, Spain
Alejandro Palacio Ensa, Spain
David Castrillón Ensa, Spain
Victor Gómez Ensa, Spain

Enrique Gómez Ensa, Spain
Rafael Grandal Ensa, Spain

ABSTRACT

The ENsa UNiversal ENUN 52B is a dual purpose metal cask developed by Ensa for dry storage and transportation of up to 52 BWR spent fuel assemblies, to meet the site-specific interim storage requirements of Sta. Ma de Garoña NPP (Spain) and future transport from the plant to the Spanish centralized interim storage facility (ATC).

The ENUN 52B cask design meets the principal storage and transportation regulations for high radioactive material from the Spanish Government and the Spanish nuclear authority (CSN). In addition, the ENUN 52B has been also designed to comply with safety standards from the IAEA, regulations from the US Code of Federal Regulations and recommendations from the US Nuclear Regulatory Commission.

The cask consists of a single carbon steel shell with structural, containment and gamma shielding capabilities. The closure system is constituted by two bolted lids separated by a pressurized helium gap for pressure and continuous leaks monitoring. The spent fuel assemblies are accommodated in the basket, which is assembled through an interlock cell structure made of stainless steel and MMC plates.

Structural performance of the ENUN 52B cask in the tipover accident scenario of storage, 0.381m drops accident scenario of storage, 1m drop onto a punch accident scenario of transport, as well as penetration impacts in normal condition of storage and transport, have been simulated by state-of-the-art explicit transient finite element methods and evaluated against the requirements of the ASME Boiler and Pressure Vessel Code [1], [2]. For the analyses of the accident impact scenarios, the finite element models consisted of the complete package modelled in detail and in three dimensions, to take into account the complex interaction between the components and the non-linearity's in the cask geometry, the material behaviour and overall cask behaviour.

This paper presents the analysis methodology, modelling technique and evaluation methodology in the analyses of the impact events for the demonstration of the performance of the ENUN 52B in the application for competent authority approval as a dual purpose cask. As

an example, analysis results, package response and evaluation results of the base down drop accident specified under the storage regulation are also described in this paper.

INTRODUCTION

The ENUN 52B is a dual purpose metal cask developed by Ensa for the dry storage and transportation of up to 52 BWR spent fuel assemblies, to meet the site-specific interim storage requirements of Sta. Ma de Garoña NPP (Spain) and future transport from the plant to the Spanish centralized interim storage facility, most commonly known as ATC as per the Spanish denomination 'Almacén Temporal Centralizado'.

Since the ENUN 52B cask has been initially designed to be licensed in Spain, it has to meet the regulations from the Spanish Government and the Spanish nuclear authority (CSN) regarding storage and transportation of high radioactive material. In addition, it has also been designed to satisfy the requirements of the international safety standards from the IAEA and regulations and recommendations from the Code of Federal Regulations and the Nuclear Regulatory Commission, both from the United States of America. Therefore, regarding storage of radioactive material, the ENUN 52B cask meets the following principal standards: IS-20 [3], IS-29 [4], IAEA SSG-15 [5], 10 CFR72 [6] and NUREG-1563 [7]. Regarding transportation of radioactive material, the ENUN 52B cask meets the following principal standards: ADR 2013 [1], RID 2013 [9], IAEA SSR-6 [10], 10 CFR71 [11] and NUREG-1617 [12].

Ensa has commissioned Arup to perform the analyses and evaluation with the aid of explicit transient finite element analysis, to demonstrate the structural performance of the cask in the following scenarios:

a) Analyses of the Accident Storage Conditions:

   - Cask tipover onto the reinforced concrete floor of the interim storage facility.
   - Axis vertical drop onto the base from 0.381m height, onto the reinforced concrete floor of the interim storage facility.
   - Centre of gravity over base edge drop from 0.381m height, onto the reinforced concrete floor of the interim storage facility.
   - Axis horizontal drop from 1m height, onto the reinforced concrete floor of the interim storage facility.

b) Analyses of the Normal and Hypothetical Transport Conditions:

   - Penetration impact under the Normal Conditions of Transport.
   - 1m height puncture drop, of the Hypothetical Accident Condition of transport.

All the analysis explained below were included into Arup's structural analysis report of the ENUN 52B cask [13], and are part of the Topical Safety Analysis Report (storage) [14] and the Safety Analysis Report (transportation) [15] of the ENUN 52B cask, that have been submitted by Ensa to the Spanish nuclear authority (CSN) for the licensing of the ENUN 52B as a dual purpose cask to be safely used in Spain.

DESCRIPTION OF THE CASK

The ENUN 52B cask consists of a single inner carbon steel shell (forging) with structural, containment and gamma shielding capabilities. The bottom of the cask is a carbon steel plate fabricated in the same material and welded to the inner shell.

The closure system is constituted by two bolted lids made of carbon steel, separated by a pressurized helium gap for pressure and continuous leaks monitoring. The bolting system allows the easy retrieval of the cask in case of an accident, and the reutilization of the cask for further transportations or fuel dry storage. The inner lid includes two penetrations with appropriate ports for draining, venting and helium pressurizing tasks performed during the cask fuel loading and unloading operations. The outer lid includes one single penetration where the pressure transducer is connected for pressure monitoring in the space between both lids during cask storage, in order to detect leaks from the inner cavity. The cask sealing lids are assured by double metal gaskets in all cask lids. The inner shell, the bottom plate and the inner lid constitute the containment barrier of the ENUN 52B cask.

The spent fuel assemblies are accommodated inside the basket of the cask, which is assembled through an interlock cell structure made of stainless steel and MMC plates. MMC is the acronym of ‘Metal Matrix Composite’, a composite material made by powder metallurgical, with a matrix of aluminium alloy and boron carbide. This material performs neutron absorption and guarantees the maintenance of the subcriticality condition of the fuel accommodated in the cask. Surrounding the interlock cell structure are assembled the aluminium basket guides, that contribute to the fuel decay heat dissipation and constitute the transition between the square shape of the basket interlock cell structure and the rounded shape of the inner shell.

The inner shell of the cask is surrounded by aluminium profiles called fins, which also contribute to the fuel decay heat dissipation. Neutron shielding material, a solid synthetic resin, is accommodated within the fins. The fins and the neutron shielding material are confined by the outer shell, a rolled plate closed by upper and lower rings that constitute the outermost side surface of the cask

The cask has four trunnions bolted to the inner shell, the two upper ones for lifting operations and the lower ones for handling operations.

Finally, two impact limiters have been also specifically designed for the ENUN 52B cask, and are bolted to the outer lid and the bottom of the cask during transportation. They are constituted by a stainless steel envelope with polyurethane foam poured inside that performs energy absorption in case of any accidental cask drop.

The main components of the ENUN 52B cask are detailed in Figure 1.

Figure 1 Main components of the ENUN 52B Cask

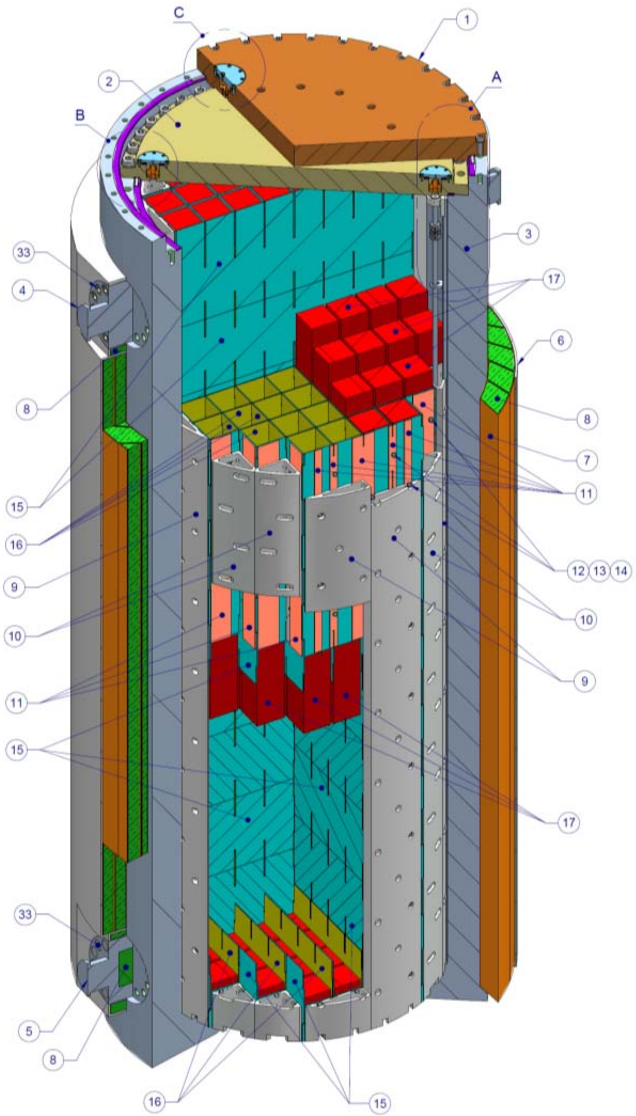

Item	Description
1	Outer lid
2	Inner lid
3	Cask body
4	Upper trunnions
5	Lower trunnions
6	Outer shell
7	Fins
8	Neutron shielding
9, 10	Basket guides
15	Stainless steel interlock cell structure
16	MMC interlock cell structure
17	Fuel assemblies

FINITE ELEMENT MODEL OVERVIEW

One finite element (FE) model, with appropriate initial orientations and velocities, was used for the analysis of all the scenarios corresponding to Accident of Storage Condition. Reduced models were used for the analysis of the specific events under Normal and Hypothetical Accident Transport Conditions.

The full model represented the entire cask ENUN 52B cask and consisted of 2.25 million elements. The analyses were carried out using the FE code LS-Dyna version 971.

The mesh of the upper part of the ENUN 52B finite element model is shown below

.

Figure 2 Mesh of the Upper Part of the ENUN 52B Finite Element Model

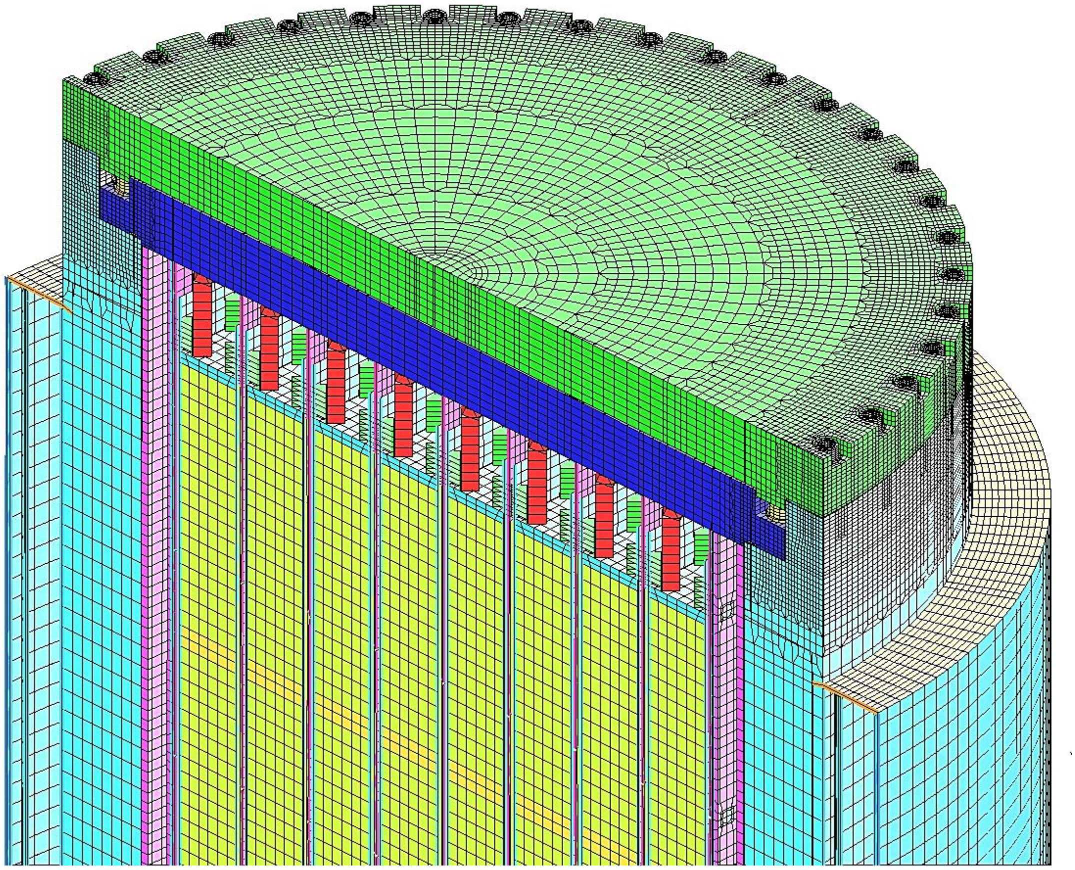

General Modelling Principles

The finite element model of the cask was designed according to the following principles:

1. The specific capabilities and limitations of the LS-Dyna solver were taken into account.
2. Mesh refinement is appropriate for the purpose of the analyses.
3. The mesh is more refined in areas of higher stress gradient and deformation gradient, and areas of smaller geometrical details.
4. The mesh is more refined in areas where a higher level of accuracy in the modellization and the analysis was required.
5. Identical mesh was used for identical components loaded with similar loadings.
6. Identical mesh was used for repeating geometry at lid-cask body interface.
7. Identical mesh was used for components that could deflect simultaneously.

8. The element quality in terms of warpage, internal angle and aspect ratio was taken into account. The aspect ratio of elements is as close to 1 as possible and no more than 3, unless unavoidable.

9. For curved surfaces that are adjacent to each other, the mesh was matched on adjacent surfaces.

Modelling of the Bolts

As explained in the cask description, the ENUN 52B has a closure system with two bolted lids. The inner lid is attached to the cask body by means of 44 M36 bolts and the outer lid is also attached to the cask body by means of 44 M27 bolts. The bolts were modelled in the finite element model through fully integrated selectively reduced eight noded brick elements, as seen in Figure 3. Threaded parts of the bolts were not modelled in detail but, based on tensile stress area of the cross section, they were "meshed in" with the mesh of the cask body. All the bolts within each set of bolts (i.e. all the inner lid bolts and all the outer lid bolts) were modelled with an identical mesh. Bolts cross sections were modelled as regular polygons with 16 sides and 32 elements in the sections, as seen in Figure 3.

Figure 3 Meshes of the Inner Lid and Outer Lid Bolts

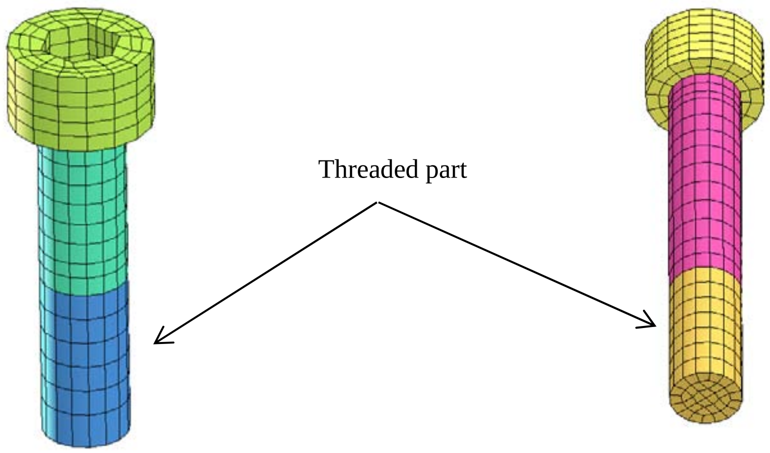

Inner lid bolt **Outer lid bolt**

Modelling of the Cask Body

The cask body was also modelled entirely with fully integrated selectively reduced eight noded brick elements. The mesh was designed starting and taking into account the meshes of the bolts, the distances between the bolt holes, the distances between the holes and the curved edges, and the location of the metal gasket seals. Nine elements was used from bolt centre to bolt centre for the inner lid interface, and thirteen elements for the outer lid interface. Identical mesh was used for repeating units, except the elements on symmetry plane that were splitted into two to facilitate "section viewing". The nodes were evenly spaced along seal line and at edges.

The mesh coarsened away from top of the cask to bottom in order to economise on the total number of elements, as seen in Figure 4. It was refined again towards the base.

These different mesh refinements are considered sufficient according to Arup's experience, to simulate the cask behaviour for this type of events.

Figure 4 Mesh Refinements in the Cask Body

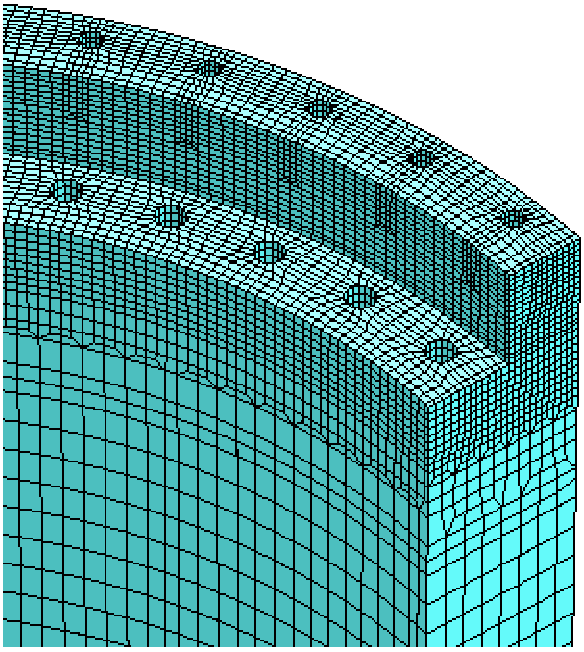

Modelling of the Lids

The inner and outer lids that constitute the closure system of the cask were also modelled with fully integrated selectively reduced eight nodded brick elements. In addition to the geometry of the lids themselves, the mesh of the bolts and the mesh of the body were also taken into account in the design of the mesh. Bolt holes were modelled with the same number of elements around the perimeter as the mesh of the bolt shanks (see Figure 5 and Figure 6).

The mesh around the curved interface with the body, matched the mesh of the cask body in order to minimise spurious stress patterns when they are in contact. The mesh was most refined around the perimeter of the lid (around the bolt holes and the interface with the body) and coarsened towards the middle, both in the through thickness direction and in hoop direction.

The metal gasket seals of the lids were modelled with non-linear springs. Along the gasket seal centre line, nodes on the lid matched the nodes on the cask body.

Figure 5 Mesh Details of the Inner Lid

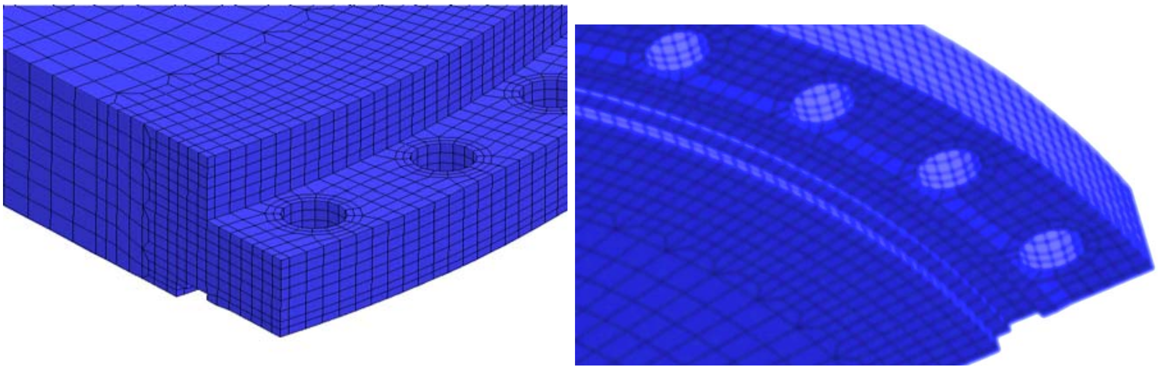

Figure 6 Mesh Details of the Outer Lid

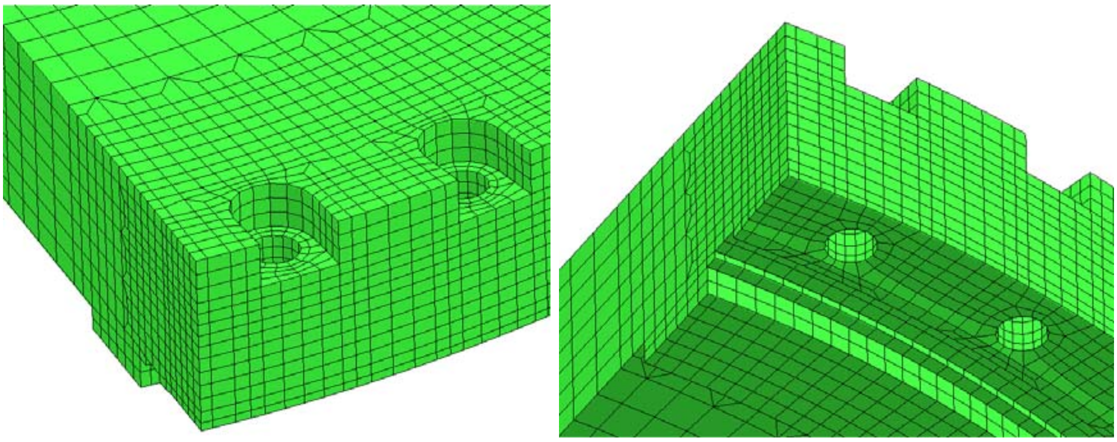

The assembled model of the cask body, the inner and outer lids, bolts and washers are shown in a section through the bolts in Figure 7. It shows the different mesh refinements of the different components and the way they interface each other.

Figure 7 Assembled Finite Element Model of Cask Body, Lids and Bolts

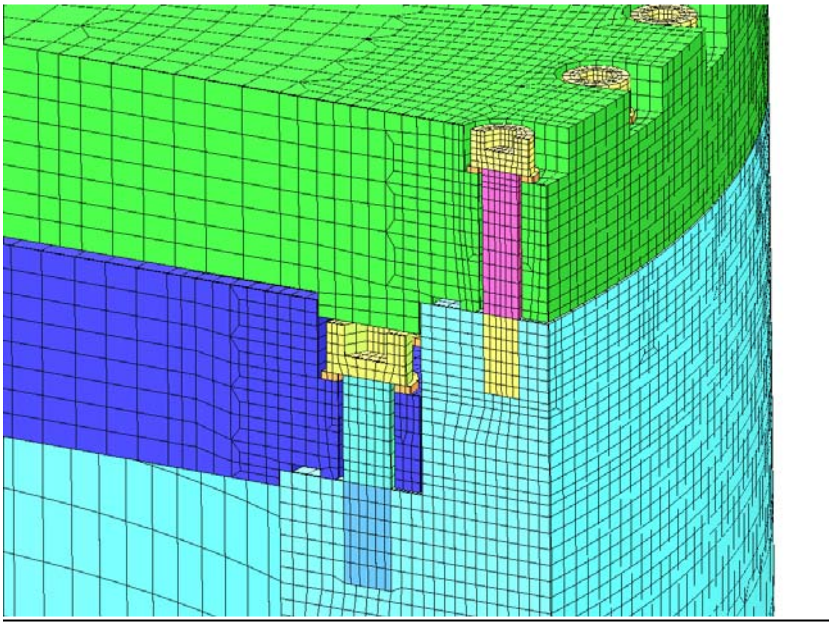

Modelling of the Basket

The basket of the ENUN 52B cask consists of a grid of stainless steel and MMC plates arranged in an interlock cell structure, as seen in Figure 8. The basket rails are installed around the perimeter of the interlock cell structure to make up the circular cross section and are bolted to the strips. They are connected by means of threaded bars together along the height to strips in the periphery of the interlock cell structure, which are welded to the stainless steel plates. The basket rails are extruded aluminium profiles with a nominal wall thickness of 15mm and narrowing down to 10mm at the cut out for the stainless steel strips. The components that constitute the basket are shown in Figure 9.

Figure 8 Illustration of the interlock cell structure of the Stainless Steel Plates in the Basket

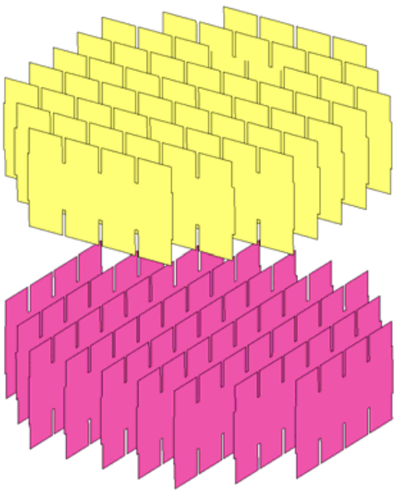

Figure 9 Components in the Basket

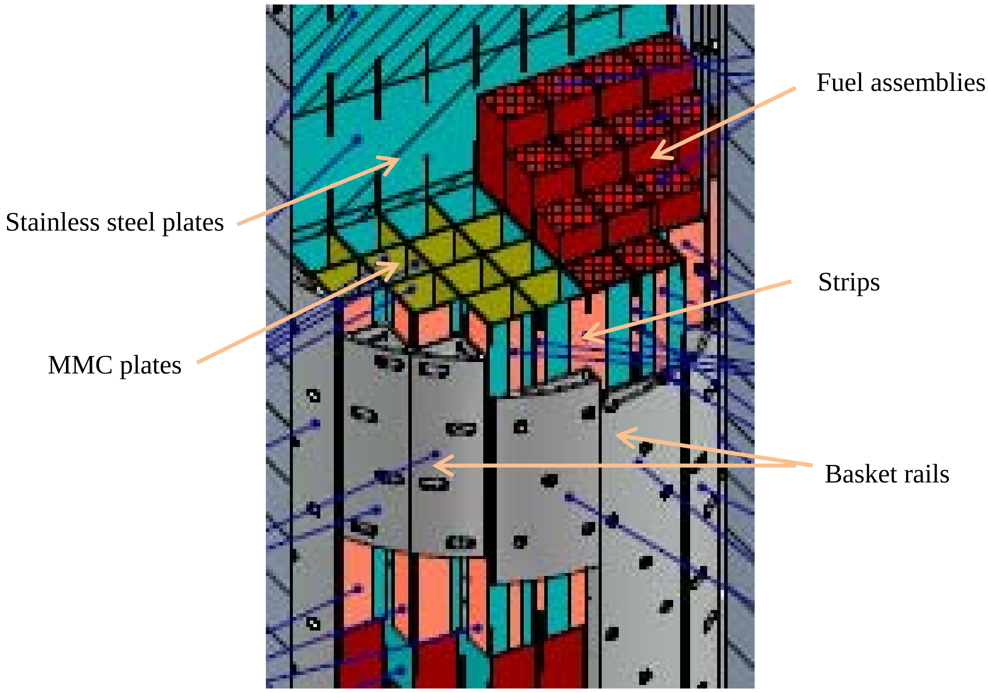

An important consideration in the modelling of the basket rails is the choice of element type: solid elements, thick shell elements, or thin shell elements.

In LS-Dyna, thick shell elements are difficult to use and results may not be robust.

Modelling with thin shell elements would imply that much of the geometric details of the basket rails would be lost. The details are considered important for the basket plates in terms of loading, support, and hence deflection and stresses. If the basket rails are modelled with thin shell elements, their interaction with the cask body inner wall and with the basket plates would be imprecise.

If they are modelled with solid elements, their complex geometry can be modelled accurately. The disadvantage is that few elements can be used in the through thickness direction because of the small thickness (15 and 10mm), and the associated problem with the aspect ratio and the number of elements that need to be used as a result.

In side drop and tipover events, the basket rails spread onto the inner wall of the cask body, and the primary loading on the basket rails would be compressive. Where there could be bending, they would work in parallel with the basket plates. In addition, no stress limit was set for the basket rails since no structural credit has been applied by Ensa to this component during the design phase. In conclusion, one layer of fully integrated selectively reduced solid elements was deemed adequate for the modelling of the basket rails. Bending stiffness would be slightly over-estimated but this would lead to higher loading in the basket plates and results would be conservative. In vertical drop events, the role of the basket rails is minor.

The mesh of the basket rails was designed such that around the perimeter, it matched the mesh of the cask body (see Figure 10) in order to minimise spurious stresses due to mesh mismatch. In the height direction, roughly two elements were used in the basket rail to one element in the cask body to maintain the required aspect ratio. Identical basket rails were modelled with identical mesh.

Figure 10 Cross Sectional View of the Meshes of the Basket Rails and the Cask Body

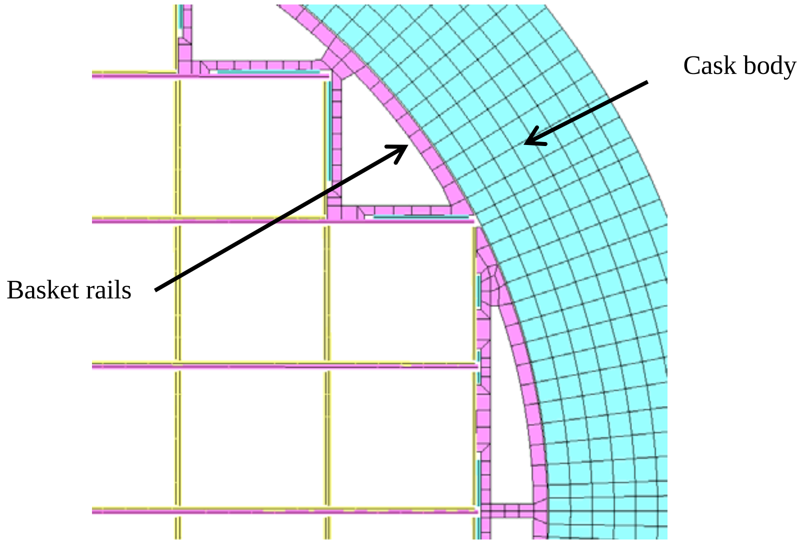

The stainless steel plates and the MMC plates of the interlock cell structure were modelled through thin shell elements. In the height direction, they were modelled with a mesh that matched that of the basket rails. In plan, the stainless steel plates that are at the perimeter were modelled with a mesh that matched the mesh of the stainless steel strips and the geometry of the basket rails. The spans of the stainless steel plates that are "free" (i.e. not attached to the basket rails) were modelled with a finer mesh of 12 elements across the cell, to capture the deflection behaviour of the plates.

The MMC plates were modelled with a mesh that matched the mesh of the adjacent stainless steel plates.

The interlocking slots in the stainless steel plates and the MMC plates were modelled explicitly. Interfaces between the stainless steel plates, between the MMC plates, and between the stainless steel and the MMC plates were modelled with contact surfaces, and consisted of an array of complicated edge to edge contacts, edge to face contacts and face to face contacts. The meshes of the different components that constitute the basket assembly is shown in Figure 11.

Figure 11 Mesh of the components that constitute the Basket Assembly

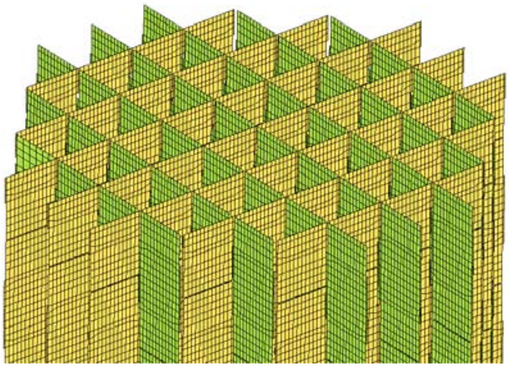

Mesh of the Interlock Cell Structure
(Stainless steel plates+ MMC plates)

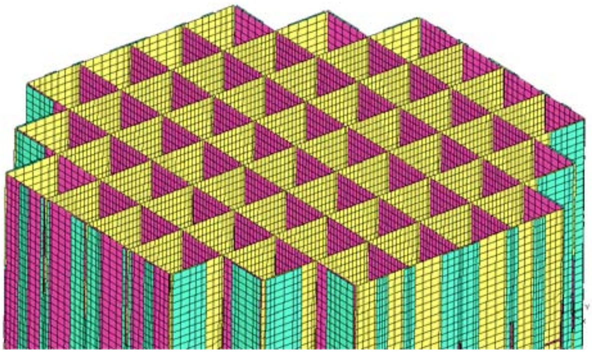

Mesh of the Interlock Cell Structure + Perimeter Strips

View from top

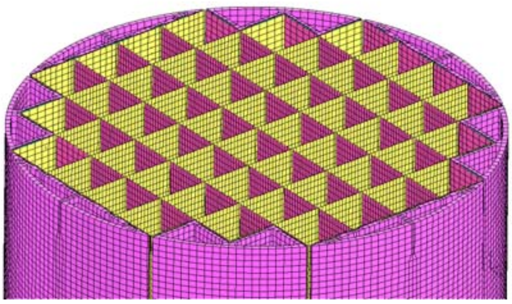

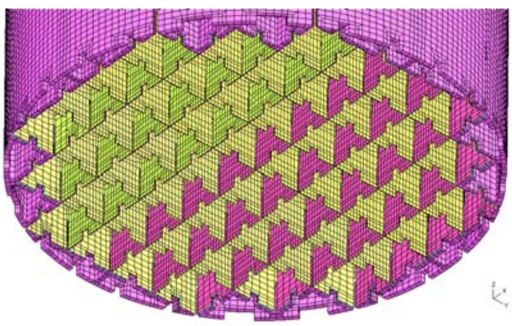

View from bottom

Mesh of the Interlock Cell Structure + Perimeter Strips + Basket Rails

Modelling of the Fuel Assemblies

The ENUN 52B cask has been designed to allocate BWR fuel assemblies of General Electric designs GE-6 and GE-7. Each fuel assembly consists of 62 fuel rods and 2 water rods, secured by 7 spacers, an upper and a lower tieplates, and enclosed on the outside by a fuel channel.

Each fuel assembly was modelled with a "smeared" properties model, with equivalent mass and stress/strain properties to provide a realistic loading onto the basket and the cask, but not for detailed prediction of the impact response on the fuel assemblies themselves. The assembly of fuel rods, tie plates and spacers was modelled with a block of solid elements with smeared properties. Tie plate handles and tripod were modelled with beam elements and fuel channel was modelled with thin shell elements. The finite element model that represents the fuel assemblies is shown in Figure 12.

Figure 12 Finite Element Model of the BWR Fuel Assemblies

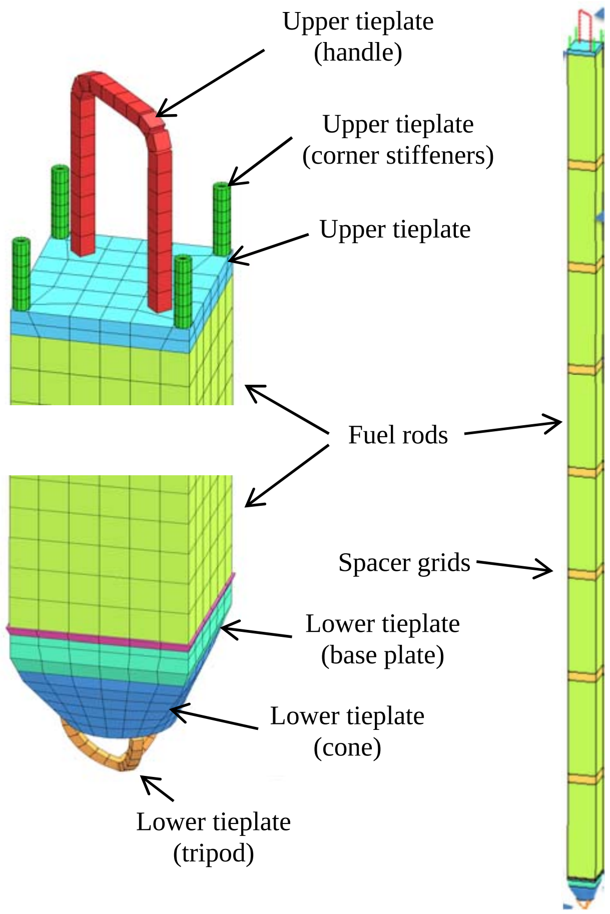

Modelling of the Impact Target

The impact target is the concrete pad of ISFSI of Sta. Ma de Garoña NPP. It is constituted by a 600mm thick reinforced concrete placed, with two layers of reinforcement steel bars, placed on bedrock. The reinforcement steel bars have a diameter of 32mm spaced 200 mm in orthogonal directions. Between the upper layer of the steel bars and the ISFSI pad outer surfaces there are 60mm of concrete cover.

The concrete was modelled with eight nodded brick elements. The reinforcement steel bars were modelled with beam elements. The interaction between the beams and the brick elements was achieved with LS-Dyna's *CONSTRAINED_ LAGRANGE_IN_SOLID facility.

Different target models were used for each impact scenario: axis vertical, axis horizontal and centre of gravity over base edge. For each of the three different impact target models, the mesh was designed such that the solid elements mesh matched the cask profile projected onto target. As an example, the finite element model of the impact target for the vertical base down drop analysis is shown in Figure 13**.**

Figure 13 Model of the impact target for the Vertical Base down Drop Analysis

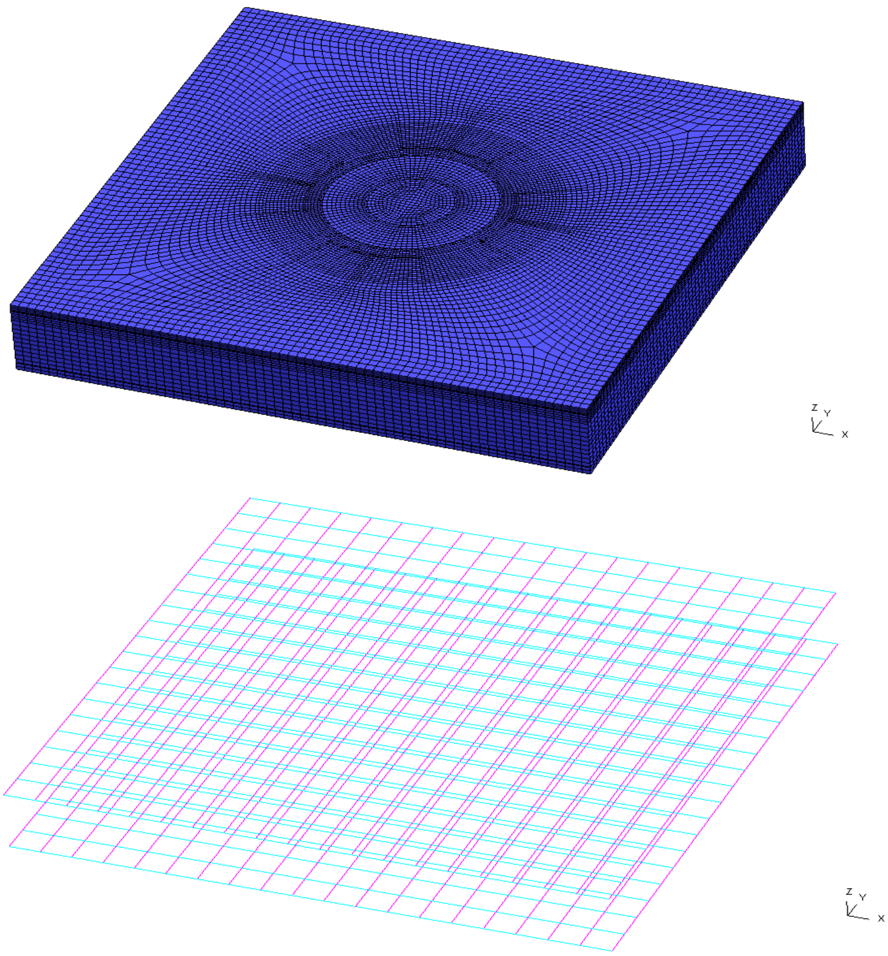

Initial Conditions in the Analysis

The following initial conditions were applied for the complete cask finite element model before launching each analysis:

- Bolt pre-stress.
- Hot condition temperature distribution in the cask components. These data was obtained from thermal simulations of the ENUN 52B cask performed by Ensa.
- Maximum internal pressure in the cask cavity.
- Initial velocity and orientation with respect to the impact target.
- Gravity loading during impact.

The following initial conditions were applied to the model in stages:

1. Bolt pre-stress was applied to the model by dynamic relaxation.
2. Hot condition temperature distribution and internal pressure in the cask cavity were applied by transient analysis.
3. Initial velocity was applied and transient analysis carried out

ANALYSIS OF BASE DOWN DROP

Among the range of storage and transportation impacts performed, the analysis of the vertical axis base down drop is summarised below. This event forms part of the Accident Storage Conditions.

Analysis Set Up

The cask was oriented with the longitudinal axis perpendicular to the target. The bottom of the cask model was located close to the target at the start of the analysis. The whole model was given an initial velocity of 2.734m/s in a direction perpendicular to the target, representing the initial impact velocity after a drop from 0.381m.

At the start of the analysis, the basket and fuel assemblies were resting on the base of the inner cavity of the cask as it would under gravity. The basket was located central to the cask body inner cavity and each fuel assembly was also located central to its basket cell. The model configuration for the base down drop analysis is shown in the figure below.

Figure 14 Initial Configuration of the Cask Model for the Base Down Drop Analysis

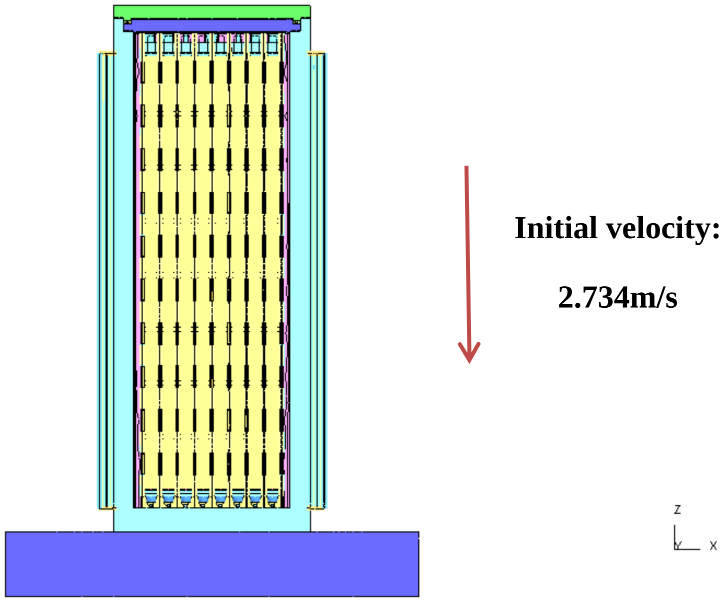

Analysis of the Cask Dynamic Response

In order to illustrate the behavior of the cask inner shell (body), displacement time histories in the Z direction (i.e. vertical axis) from three measurement points on the body as shown in Figure 15 (near the top of the outside of the cask body on the level of the inner lid gasket seat (N1), near the bottom of the outside of the cask body just below the base of the neutron shielding (N2), and in the middle on the upper surface of the base (N3)) have been extracted from the analysis, and are shown in Figure 16.

N2 started to slow down earlier and came to a stop before than N1. The difference in displacement between N1 and N2 indicates that the cask body shortened by about 2mm at maximum displacement. As the body rebounded, the overall height of the body recovered, and oscillated as it rebounded. N3 came to a stop earlier and displaced less than N2. It flexed upwards with respect to the edge and then oscillated.

Figure 15 Vertical Displacement Measurement Points in the Cask Body, in Base Down Drop Analysis

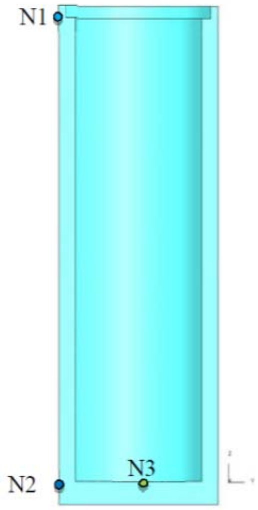

Figure 16 Vertical Displacement Time Histories of the Measurement Points in the Cask Body in Base Down Drop Analysis (mm vs. s)

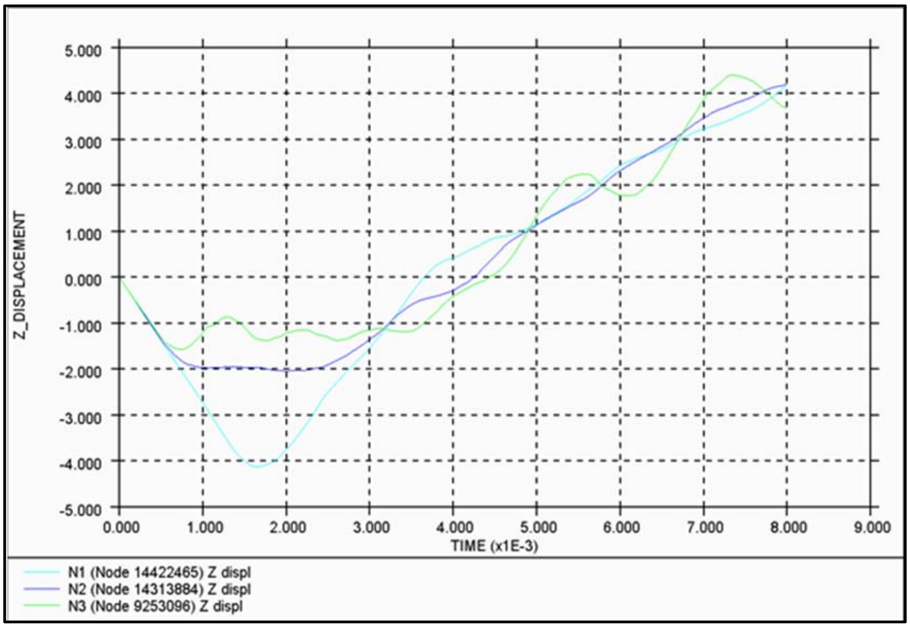

In order to illustrate the behaviour of the closure lid system during the impact, displacement time histories in the Z direction (i.e. vertical axis) from the three measurement points, two on the lids and one on the body, as shown in Figure 17 (N1, N4 and N5), have been also extracted from the analysis, and are also shown in Figure 17.

The lids experienced their largest deflections considerably later than the top of the body, in fact, when the top of the body was already rebounding. The two lids deflected at different rates to different extents, due to difference in bending stiffness, mass and support diameter. The lids rebounded from a "dished" deflection to a "domed" deflection, and went through cycles of oscillation as the package rebounded.

Figure 17 Vertical Displacement Time Histories of the Measurement Points in the Closure System in Base Down Drop Analysis (mm vs. s)

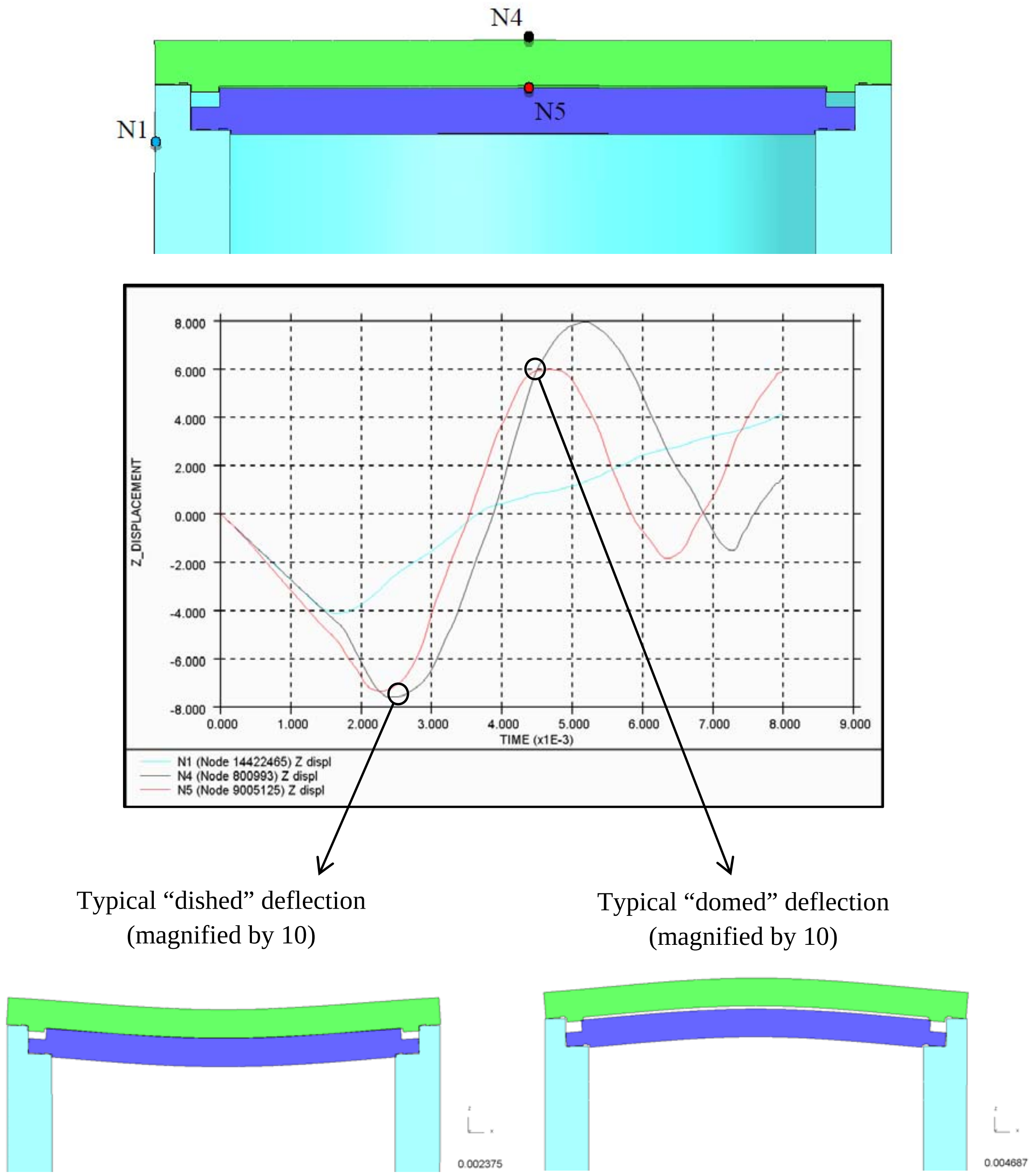

To illustrate the bending nature of the lids during the “dished” and “domed” deflections already indicated, X direct stress distributions in the lids on a XZ cross section at the time of maximum “dished” deflection and at the time of “domed” deflection, are shown in Figure 18**.**

Figure 18 Direct Stresses Distributions in the Inner and Outer Lids in the Base Down Drop Analysis (MPa)

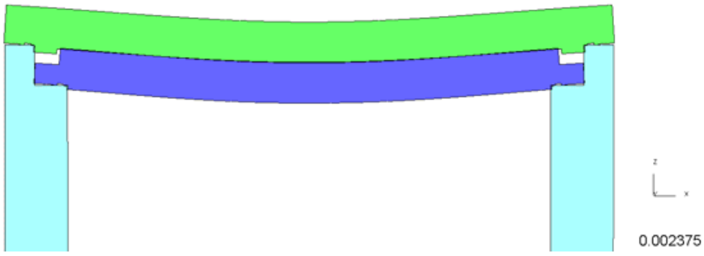

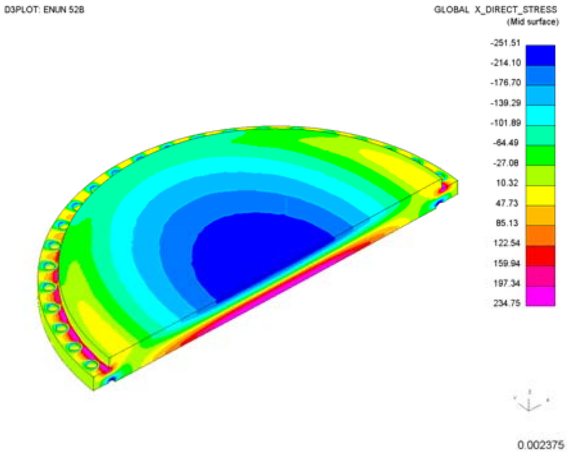

Inner lid bending stresses at "dished" deflection

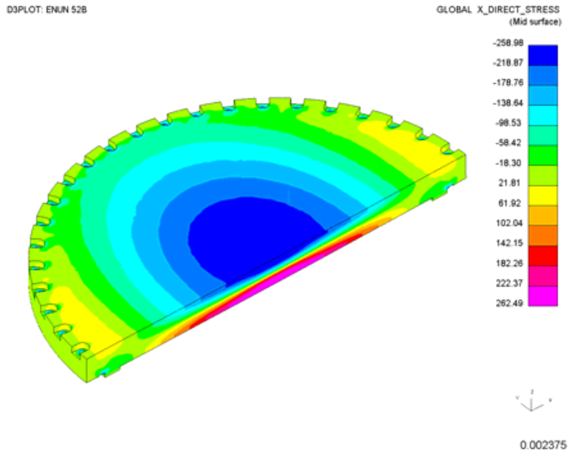

Outer lid bending stresses at "dished" deflection

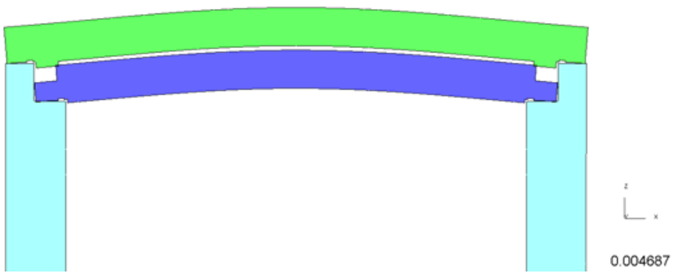

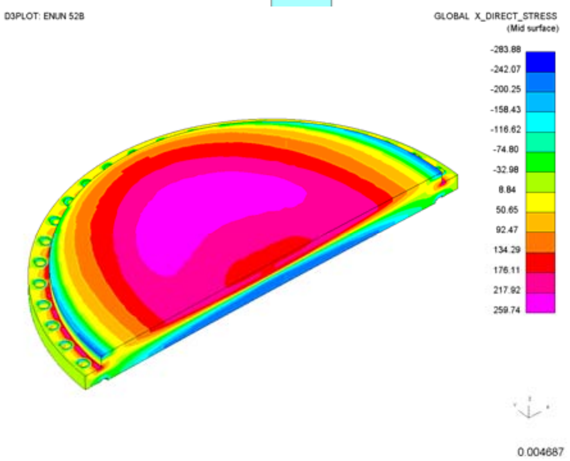

Inner lid bending stresses at "domed" deflection

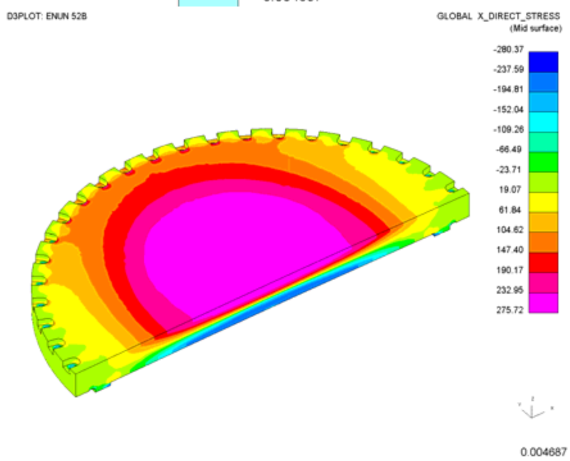

Outer lid bending stresses at "domed" deflection

When one of the lids was at a “dished” deflection, it was supported (i.e. pivoted) about the edge of the seating on the body and the lid bolts were stretched and bent as a result of a “prying” type loading. When a lid rebounded from a “dished” deflection, it jumped from the seating and it was restrained by the lid bolts. The bolts were again put into tension and experienced bending but in a different direction to that when the lid was in a “dished” deflection. These effects are shown in Figure 19**.**

Figure 19 Bolt Stress Distributions as a Consequence of Lids “Dished” and “Domed” Deflections (MPa)

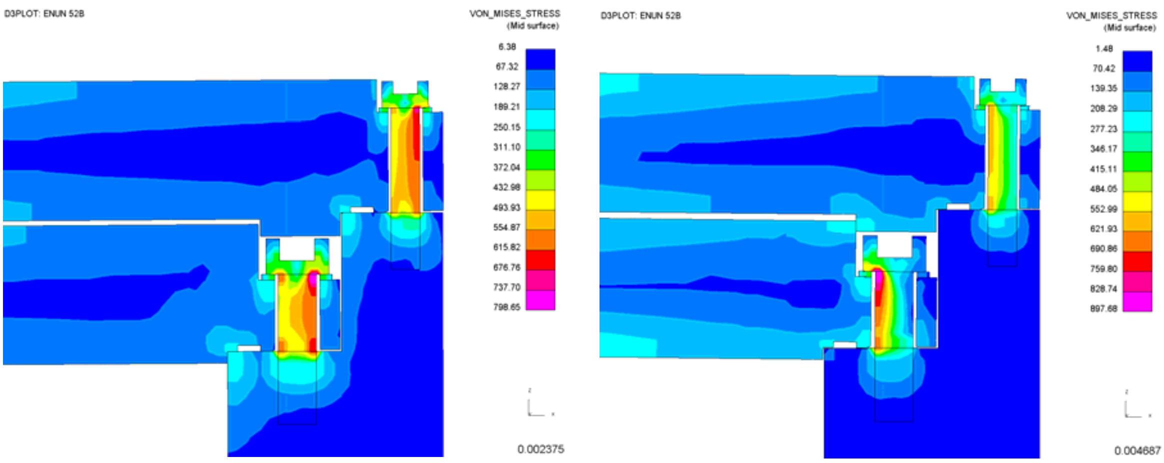

Bolt stresses at time of “dished” deflection

Bolt stresses at time of “domed” deflection

Vertical displacement time histories at the top of a typical basket rail (N6), at the top of a stainless steel plate near the middle of the axis (N7), and at the top of a fuel assembly (N8) are shown together with the displacement time history at the top of the cask body (N1) in Figure 20.

Figure 20 Vertical Displacement Time Histories of three Measurement Points in the Cask Body in the Basket (mm vs. s)

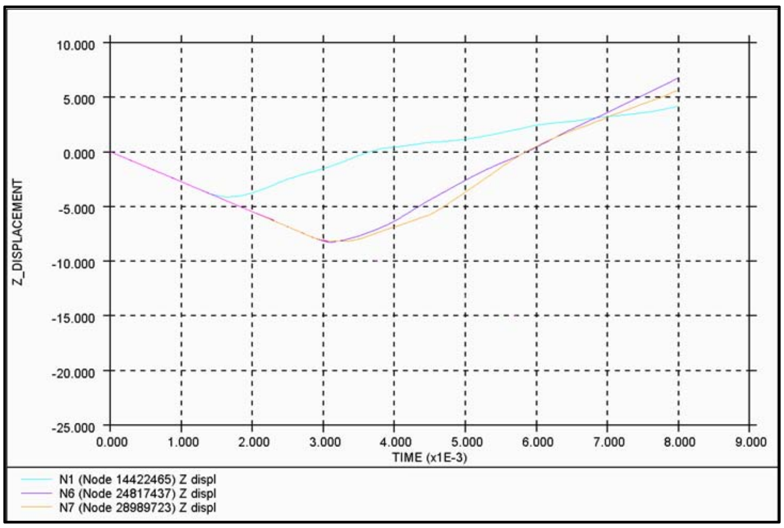

The displacement time history at the top of the basket rail is similar to that at the top of the stainless steel plate, since they are connected and are part of the basket assembly. The maximum displacement in the stainless steel plates happened much later, at 3.2ms, than that of the body due to basket's flexibility. In fact, it was still moving downwards when the body was already on its rebound.

Von Mises stress distribution in the stainless steel plates, measured at mid surface of the thin shell elements, at the time of maximum downward displacement, is shown in Figure 21. Since the inertia loading on a basket plate at the top of the basket is lowest and on a basket plate at the bottom of the basket is highest, stresses increase towards the bottom of the basket.

No contact was observed between the basket components or the fuel assemblies with the inner lid, during the entire duration of the base down drop analysis.

Figure 21 Von Mises Stress Distribution in the Basket Stainless Steel Plates (MPa)

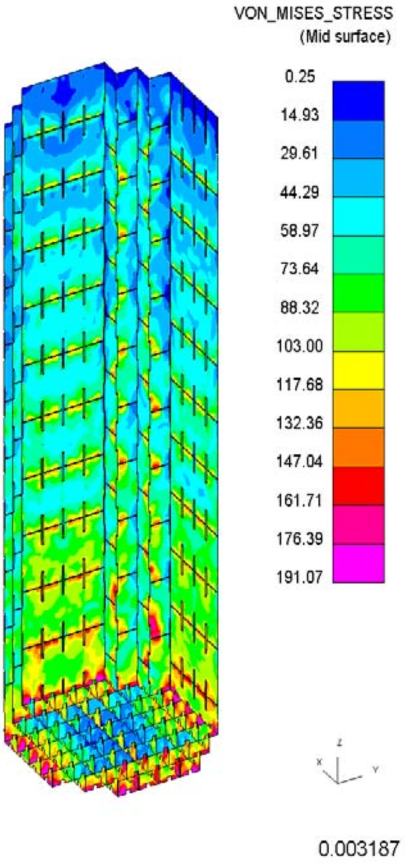

Stress Analysis of the Cask

Stress analysis of the components of the ENUN 52B cask was performed following the criteria indicated in the corresponding "Design by Analysis" paragraphs of Section III, Division 1 and Section III, Division 3 of the ASME Code [1], [2]. Loads produced in the cask due to Accident Storage Conditions are classified as Level D loads in the ASME Code criteria, except loads in the inner lid bolts that are classified as Level A loads since its failure could lead to leaks from the inner cavity [2]. Stresses calculated on each component were compared to the corresponding stress allowable limits, taking into account the material of the component and its temperature under Normal Conditions of Storage, and obtained from the corresponding section of the ASME Code.

The bounding distributions[1] of the maximum shear stress in the cask body, the inner lid and the outer lid are shown in Figure 22.

Stress analysis of the inner lid bolts has been performed through stress linearization of the most stressed bolt [2], at the bolt cross section where stress concentrations produce the highest values of the maximum shear stress: the interface area between the head and the shank of the bolt. For the outer lid bolts, average axial and shear stresses on the most stressed bolt are combined.

The comparison of the stresses calculated on the cask body, the inner lid, the outer lid and the bolts are shown in Table 1, and demonstrate that are below the allowable limits.

Finally, an analysis of the maximum lateral displacements of the stainless steel and MMC plates at the end of the base down drop impact has been performed, for the structural assessment of the basket. In Figure 23, the displacements of the plates along the global X and Y axes are shown. Results show that maximum deformations measured in the basket cells do not violate the retrievability of the fuel assemblies after the accident, as recommended by document NUREG-1536.

All these results demonstrate that the behaviour of all components that constitute the ENUN 52B cask, following the "Design by Analysis" criteria established by the ASME Code, satisfy the requirements of the corresponding regulations regarding storage of radioactive materials.

[1] Bounding distributions represent the maximum values of the max shear stress ($\tau_{máx}$) on each of the elements of the component shown, throughout the duration of the analysis.

Figure 22 Bounding Distributions of the Maximum Shear Stress in the Cask Body, the Inner Lid and the Outer Lid (MPa)

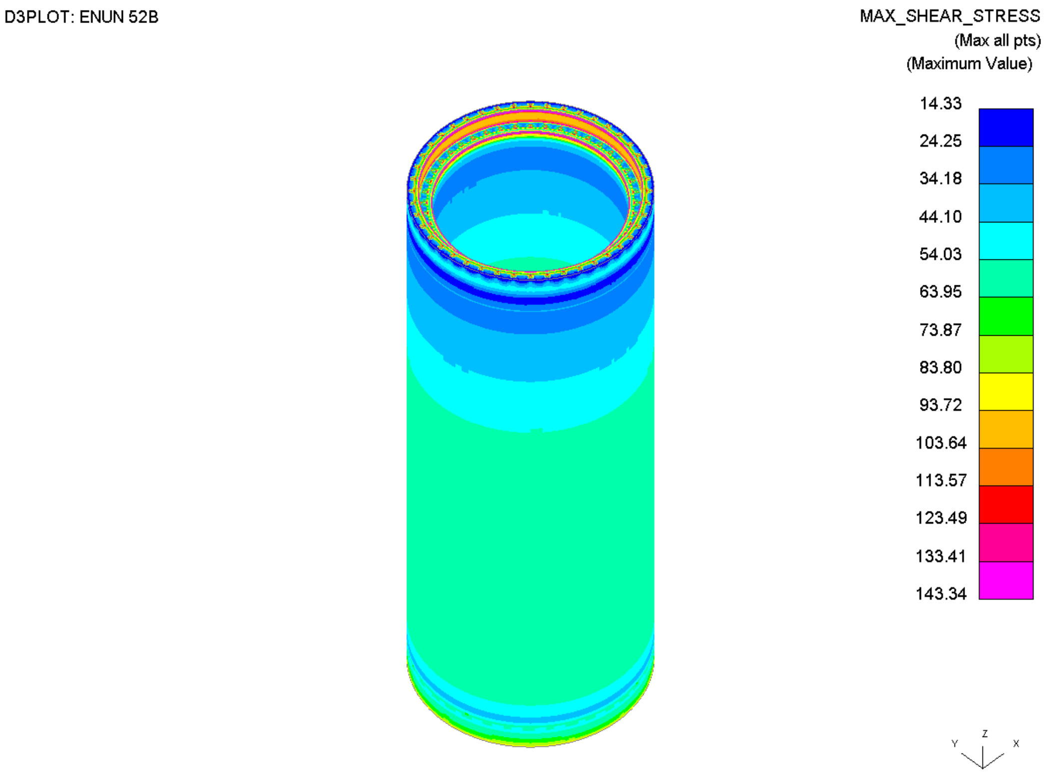

Cask body

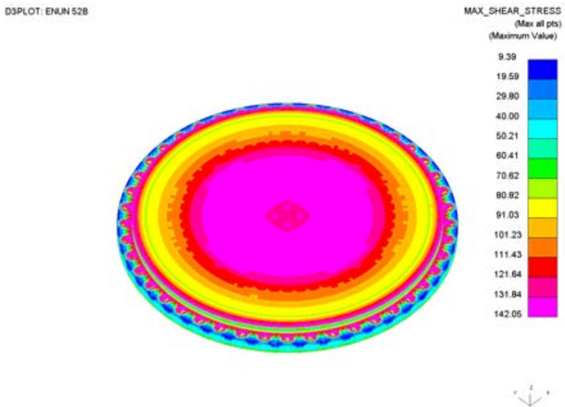

Inner lid

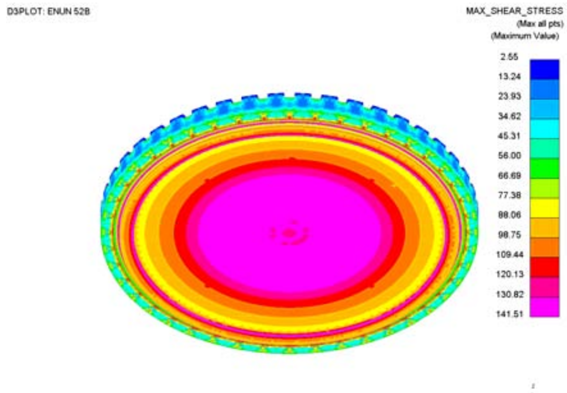

Outer lid

Table 1 Stress Analysis for the Base Down Drop Analysis [2]

Component	Stresses (MPa)		
	Allowable limit	Calculated Results	
	$0.7 \cdot S_u$	τ_{max}	SI ($2 \cdot \tau_{max}$)
Cask body	412.5	143.3	286.7
Inner lid	412.5	142.1	284.1
Outer lid	395.6	141.5	283.0

Component	Average Normal Stresses (MPa)		Average Shear Stresses (MPa)		Maximum Stress Intensity (MPa)	
	Allowable limit	Calculated Results	Allowable limit	Calculated Results	Allowable limit	Calculated Results
	$2 \cdot S_m$	σ_{med}	$1.2 \cdot S_m$	τ_{med}	$3 \cdot S_m$	SI
Inner lid bolts	670.3	335.0	402.2	25.1	1005.5	884.0

Component	Average Normal Stresses (MPa)			Average Shear Stresses (MPa)			Combined Normal and Shear Stresses (MPa)	
	Allowable limit		Calculated Results	Allowable limit		Calculated Results	Allowable limit	Calculated Results
	$0.7 \cdot S_u$	S_y	σ_{med}	$0.42 \cdot S_u$	$0.6 \cdot S_y$	τ_{med}	-	-
Outer lid bolts	798.0	1007.0	602.9	478.8	604.2	27.1	1	0.6

[2] τ_{max}: maximum shear stress; τ_{med}: average shear stress; σ_{med}: average normal stress; SI: stress intensity; S_m: design stress intensity; S_y: yield strength; S_u: tensile strength.

Figure 23 Lateral Displacements (Along Global X and Y Direction) of the Stainless Steel and MMC Plates of the Basket at the End of the Base Down Drop Analysis (mm)

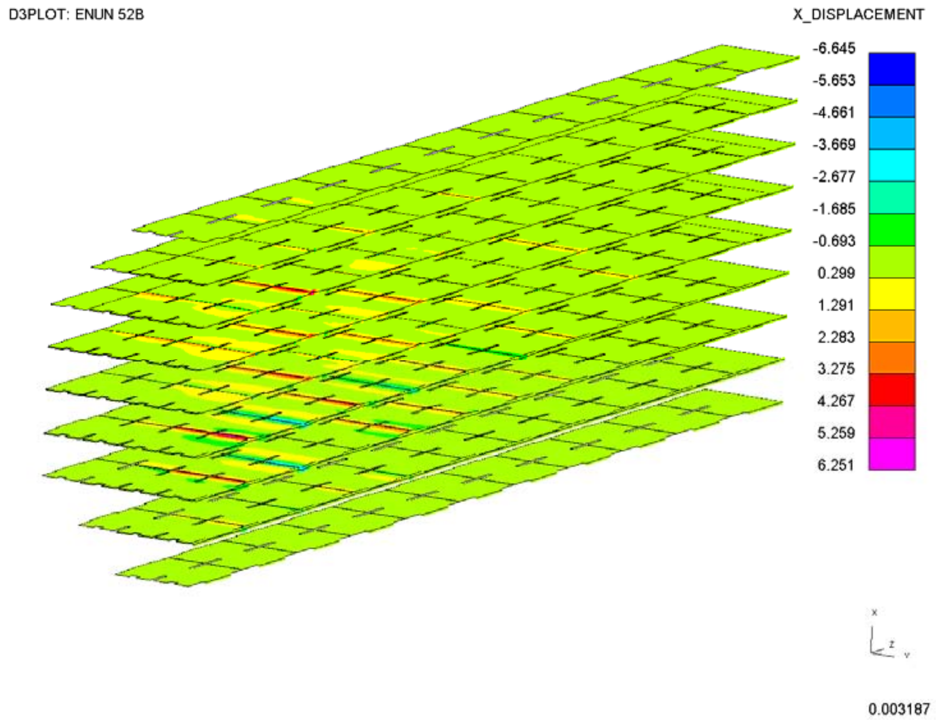

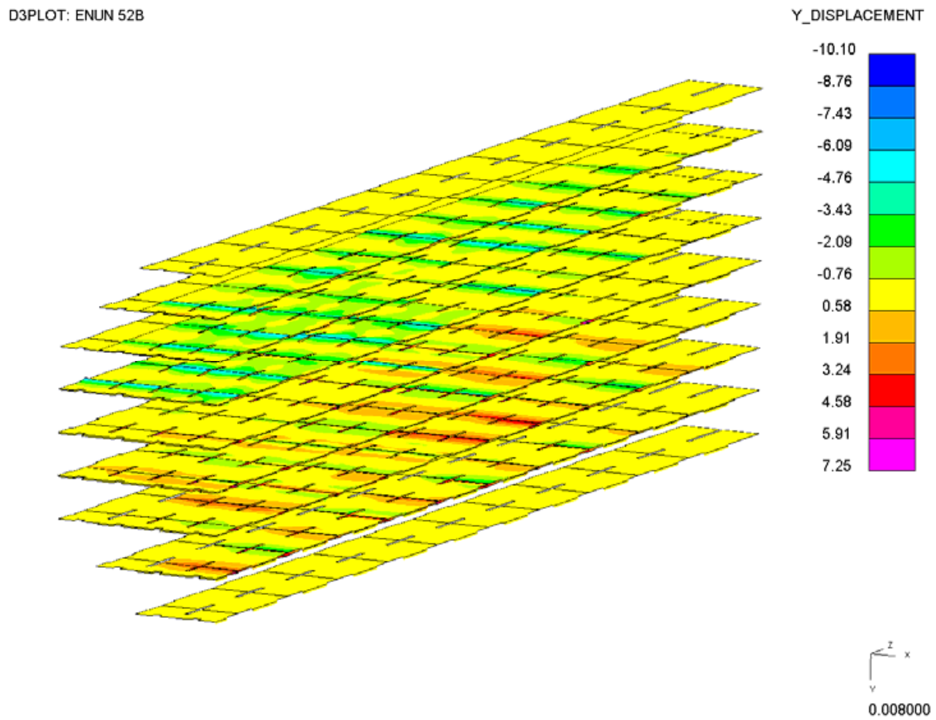

CONCLUSIONS

Ensa has commissioned Arup to perform the analyses and evaluation to demonstrate the structural performance of the ENUN 52B dual purpose metal cask, under some of the events classified under Accident Storage Conditions and Normal and Hypothetical Transport Conditions. These analyses are part of the design process to get the license of use of the ENUN 52B cask for storage and transportation of radioactive material.

Arup has developed a detailed explicit transient finite element model of the entire ENUN 52B cask. Within all the impact scenarios analysed, this paper describes the analysis results of the base down drop impact under Accident Storage Conditions.

All results presented demonstrate that the behaviour of all components that constitute the ENUN 52B cask, following the "Design by Analysis" criteria established by the ASME Code, satisfy the requirements of the corresponding regulations regarding storage of radioactive materials.

REFERENCES

[1] ASME Boiler & Pressure Vessel Code. Section III, Division 1. 2010 Edition, The American Society of Mechanical Engineers, New York, New York, USA.

[2] ASME Boiler & Pressure Vessel Code. Section III, Division 3, Containments for Transportation and Storage of Spent Nuclear Fuel and High Level Radioactive Material and Waste. 2010 Edition, The American Society of Mechanical Engineers, New York, New York, USA.

[3] Instrucción IS-20, de 28 de enero de 2009, del Consejo de Seguridad Nuclear, por la que se establecen los requisitos de seguridad relativos a contenedores de almacenamiento de combustible gastado. Boletín Oficial del Estado. Miércoles 18 de febrero de 2009.

[4] Instrucción IS-29, de 13 de octubre de 2010, del Consejo de Seguridad Nuclear sobre instalaciones de almacenamiento temporal de combustible gastado y residuos radiactivos de alta actividad. BOE nº265 de 2 de noviembre de 2010.

[5] IAEA Safety Standards, Specific Safety Guide No. SSG-15, "Storage of Spent Nuclear Fuel", 2012 Edition, Vienna.

[6] 10 CFR 72, "Licensing Requirements for the Independent Storage of Spent Nuclear Fuel and High-Level Radioactive Waste and Reactor-Related Greater than Class C Waste", Part 72, Title 10 of the Code of Federal Regulations.

[7] NUREG-1536, "Standard Review Plan for Dry Cask Storage Systems", U.S. Nuclear Regulatory Commission, Rev. 1, July 2010.

[8] ADR 2013, Acuerdo europeo sobre transporte internacional de mercancías peligrosas por carretera. Ministerio de Fomento, Gobierno de España. Publicado en el BOE núm. 63, de 14 de marzo de 2013.

[9] RID 2013, Reglamento relativo al transporte internacional de mercancías peligrosas por ferrocarril. Ministerio de Asuntos Exteriores y Cooperación. Publicado en el BOE núm. 91, de 16 de abril de 2013.

[10] IAEA Safety Standards, Specific Safety Requirements No. SSR-6, "Regulations for the Safe Transport of Radioactive Material", 2012 Edition, Vienna.

[11] 10 CFR 71, "Packaging and Transportation of Radioactive Materials", Part 71, Title 10 of the Code of Federal Regulations.

[12] NUREG-1617, "Standard Review Plan for Transportation Packages for Spent Nuclear Fuel", U.S. Nuclear Regulatory Commission, March 2000.

[13] Doc Ref 225864-00-02, "ENUN 52B Dual Purpose BWR Spent Fuel Cask – Safety Analyses. Explicit Transient Analyses and Evaluation", Issue 1.

[14] 9267-A, Estudio de Seguridad de Almacenamiento del Contenedor ENUN 52B, Revisión 0. Ensa, Julio 2013.

[15] 9267-T, Estudio de Seguridad de Transporte del Contenedor ENUN 52B, Revisión 0. Ensa, Agosto 2013.